MOL#66498

Monepantel allosterically activates DEG-3/DES-2 channels of the gastrointestinal nematode *Haemonchus contortus*

Lucien Rufener[1], Roland Baur[1], Ronald Kaminsky, Pascal Mäser and Erwin Sigel

Institute of Biochemistry and Molecular Medicine, University of Bern, Switzerland (R.B., E.S.). Institute of Cell Biology, University of Bern, Switzerland (L.R., P.M.). Novartis Centre de Recherche Santé Animale, St. Aubin, Switzerland (R.K.). Swiss Tropical and Public Health Institute, Basel, Switzerland (P.M.). University of Basel, Switzerland (P.M.)

1

MOL#66498

Running title:

Monepantel activates *H. contortus* DEG-3/DES-2 channels

Correspondence: Erwin Sigel

Institute of Biochemistry and Molecular Medicine

University of Bern

Bühlstrasse 28

CH-3012 Bern

Switzerland

E-mail: erwin.sigel@mci.unibe.ch

Number of text pages: 15

Number of tables: 1

Number of figures: 6

Number of references: 31

Number of words in the abstract: 246

Number of words in the introduction: 748

Number of words in the discussion: 867

Abbreviations: AAD, amino-acetonitrile derivative; GABA, γ-aminobutyric acid; GABA$_A$ receptor, γ-aminobutyric acid type A receptor; nAChR, nicotinic acetylcholine receptor.

ABSTRACT

Monepantel is the first drug of a new family of anthelmintics, the amino acetonitrile derivatives (AAD), presently used to treat ruminants infected with gastrointestinal nematodes such as *Haemonchus contortus*. Monepantel shows an excellent tolerability in mammals and is active against multidrug-resistant parasites, indicating that its molecular target is (i) absent or inaccessible in the host and (ii) different from those of the classical anthelmintics. Genetic approaches with mutant nematodes have suggested acetylcholine receptors of the DEG-3 subfamily as the targets of AADs, an enigmatic clade of ligand-gated ion channels that is specific to nematodes and does not occur in mammals. Here we demonstrate direct interaction of monepantel, its major active metabolite monepantel sulfone, and other AADs with potential targets of the DEG-3 subfamily of acetylcholine receptors. *Haemonchus contortus* DEG-3/DES-2 receptors were functionally expressed in *Xenopus* oocytes and found to be preferentially activated by choline, to permeate monovalent cations, and to a smaller extent, calcium ions. While monepantel and monepantel sulfone did not activate the channels by themselves, they substantially enhanced the late currents after activation of the channels with choline, indicating that these AADs are type II positive allosteric modulators of *H. contortus* DEG-3/DES-2 channels. Interestingly, the inactive, R-enantiomer of monepantel inhibited the late currents after stimulation of *H. contortus* DEG-3/DES-2 receptors with choline. In summary, we present the first direct evidence for interaction of AADs with DEG-3 type acetylcholine receptors and discuss these findings in the context of anthelmintic action of AADs.

INTRODUCTION

The nematode *Haemonchus contortus* is a gastrointestinal parasite of ruminants that causes substantial economic losses to sheep and cattle production worldwide. Adult worms live in the mucosa of the abomasum (the final stomach compartment of ruminants) where they feed on blood. Eggs are shed by the thousands with the feces. High worm burdens can lead to severe anemia and even death of the infected animal. In the absence of vaccines against gastrointestinal nematodes, the control of infection relies mainly on treatment with anthelmintics. However, successful control is jeopardized by the increasing occurrence and spread of drug resistant nematodes (Traversa et al., 2007; Waghorn et al., 2006; Kaplan, 2004; Love et al., 2003; Coles, 1998). Until recently, only three major classes of anthelmintics have been available: the benzimidazoles (e.g. thiabendazole), imidazothiazoles (e.g. levamisole), and macrocyclic lactones (e.g. ivermectin). Reports of multidrug-resistant *H. contortus* withstanding all these anthelmintics (Sutherland et al., 2008; Wrigley et al., 2006; Yue et al., 2003) were particularly alarming. On some properties this culminated in the termination of sheep farming (Blake and Coles, 2007; Sargison et al., 2005). Monepantel (ZOLVIX[®]) is the first new anthelmintic to be introduced for livestock for more than 27 years (Kaminsky et al., 2008a, b). Monepantel belongs to a new class of anthelmintics, the amino-acetonitrile derivatives (AAD; Ducray et al., 2008). Monepantel is able to control infections of nematode isolates resistant to all the classical anthelmintics (Kaminsky et al., 2008b), indicating that the AADs have a different mode of action.

While benzimidazoles bind to ß-tubulin and inhibit the formation of microtubuli, the majority of anthelmintics affect ion channel function of the neuromuscular synapse

(Holden-Dye and Walker, 2007). Piperazine acts as a weak GABA-mimetic, levamisole, pyrantel and morantel are nicotinic acetylcholine receptor agonists, paraherquamide is a competitive antagonist of these channels, macrocyclic lactones are positive allosteric modulators of glutamate-gated chloride channels, and emodepside acts on a post-synaptic calcium-activated potassium channel and on pre-synaptic latrophilins. Interference with synaptic signal transduction at the neuromuscular junction paralyzes gastrointestinal nematodes, and they are either killed or expelled by the intestine's peristalsis. In this context, the molecular mechanism of anthelmintic action of monepantel is of high interest. A molecular genetic approach with the nematode *Caenorhabditis elegans* indicated that the AADs, too, acted via ligand-gated ion channels: in mutagenized worms subjected to sublethal doses of AAD, loss of sensitivity was mapped to a gene encoding a putative nicotinic acetylcholine receptor (nAChR) alpha subunit, ACR-23 (Kaminsky, 2008a). Related genes were found to be involved in *H. contortus*, where loss-of-sensitivity mutants carried a panel of nonsense mutations and mis-splicing mutations in the two nAChR genes *Hco-des-2* and *Hco-mptl-1* (Rufener et al., 2009).

All these subunits – *C. elegans* ACR-23, Hco-MPTL-1, and Hco-DES-2 – are members of the DEG-3 subfamily of nAChR subunits, a clade that only occurs in nematodes. Very little is known about this subfamily. The founding member *C. elegans* DEG-3 was described to form, when co-expressed with DES-2 in *Xenopus laevis* oocytes, an ion channel gated by choline rather than acetylcholine (Treinin et al., 1998). These DEG-3/DES-2 channels are partially permeable to Ca^{2+} and in *C. elegans*, they are probably involved in chemosensation in sensory neuronal endings (Yassin et al., 2001). The ER-resident chaperonin RIC-3 not only enhanced DEG-3/DES-2 expression

(Halevi et al., 2002), it also influenced the functional properties of the DEG-3/DES-2 channel, an effect which was mimicked by an increase in the DEG-3:DES-2 ratio used during expression (Ben-Ami et al., 2005). A high DEG-3:DES-2 ratio favoured fast and near complete desensitization whereas a low DEG-3:DES-2 ratio led to slower and incomplete desensitization. To our knowledge there are no functional data on other members of the DEG-3 subfamily. Since nAChR function as homo- or heteromeric pentamers, the heterologous expression of novel channels, whose subunit composition and stochiometry is unknown, is notoriously difficult.

The finding that loss-of-sensitivity mutants of *C. elegans* and *H. contortus* carried nonsense mutations in nAChR subunits of the DEG-3 subfamily is consistent with the hypothesis that the AADs somehow activate these channels. However, there has so far been no direct evidence for action of AADs on DEG-3 type AchR channels. Here we functionally express *H. contortus* nAChR channels of the DEG-3 subfamily in *Xenopus* oocytes, with particular reference to the mode of action of monepantel (AAD-1566) and its major active metabolite monepantel sulfone (AAD-4670; Karadzovska et al., 2009). We show that the channel formed by Hco-DEG-3 and Hco-DES-2 is allosterically potentiated by monepantel and monepantel sulfone.

Material and Methods

Cloning of nicotinic acetylcholine receptor subunits from Haemonchus contortus. *H. contortus* RNA extraction, cDNA synthesis, PCR amplification of target genes and rapid amplification of cDNA ends by PCR (RACE-PCR) was performed as described (Rufener et al., 2009). Briefly, total RNA was extracted from a pool of about 50 adult nematodes and 1 µg of total RNA (DNase treated) was reverse transcribed to

cDNA using a $(dT)_{30}$ primer and SuperScript II Reverse Transcriptase (Invitrogen). The gene-specific PCRs were performed using the Expand High Fidelity PCR system (Roche). The following primers were used to amplify full-length coding sequences. For *Hco-mptl-1*: Hc-mon-1_5'_frw3 (gagggcaacaatttccttca) and *Hc-mon-1*_3'end_rev1 (tgactagagagggcgatcttg). For *Hco-des-2*: NheI_*des-2*_frw1 (ggcggctagccgctcctcccctac ctacta) and XhoI_*des-2*_rev1 (ggcgctcgagcatatcactgatttttccatcgtt). For *Hco-deg-3*: NheI_*deg-3*_frw1 (ggcggctagcatgcgactacatgaaacctcg) and NotI_*deg-3*_rev1 (ggcggcggccgcttagaagaatgcctcgtctgg). For *Hco-ric-3*, a rapid amplification of cDNA ends by PCR (RACE-PCR) was performed using internal reverse primers *Hco-ric-3*_rev1 (acctcatttgcaccttctgc) and *Hco-ric-3*_rev3 (tcttgctcattgcctcttca) combined with splice leader sequence 1 (ggtttaattacccaagtttgag) to obtain the 5' UTR, respectively internal forward primers *Hco-ric-3*_frw1 (ggtttggttgtgggtgtgat) and *Hco-ric-3*_frw2 (tccaatgctgatgagcctact) combined with a poly-dT primer for the 3' UTR of the transcript. The gene-specific primers were designed using the Primer3 software (http://frodo.wi.mit.edu/). The full-length *Hco-ric-3* coding sequence was amplified using primers NheI_*ric3*_frw1 (ggcggctagcatgcctgttcacgggcga) and XhoI_*ric3*_rev1 (gaccacttccacgctttcatctcgagcgcc). The amplicons were analyzed on 1% agarose gels, excised, gel-purified using the Wizard® SV PCR Clean-Up kit (Promega), and cloned into pCR®II-TOPO® (Invitrogen) or pGEM-T easy (Promega; only for *Hco-mptl-1*). Plasmid DNA was purified using the QIAprep Spin Miniprep Kit (Qiagen) and sequenced using the standard M13 forward and reverse or T7 and SP6 primers at Microsynth (www.microsynth.ch). At least three clones of each construct were analysed and aligned in order to find a 'consensus-like' clone. The selected inserts were then subcloned into pcDNA3.1(+) (Invitrogen) via the restriction sites inserted in the

primers, respectively via NotI and SpeI for *Hco-mptl-1*. Plasmid DNA was purified with an EndoFree®Plasmid Purification Kit (Qiagen). The *H. contortus* genes were named following the suggestions by Beech et al. (2010).

Expression of Haemonchus contortus DEG-3/DES-2 receptors in Xenopus oocytes. Capped cRNAs were synthesized (Ambion) from the linearized vectors containing the different subunits. A poly-A tail of about 400 residues was added to each transcript using yeast poly-A polymerase (USB). The concentration of the cRNA was quantified on a formaldehyde agarose gel using Radiant Red stain (Biorad) for visualization of the RNA with known concentrations of RNA ladder (Invitrogen) as standard on the same gel. The cRNAs were dissolved in water and stored at –80°C. Isolation of oocytes from the frogs, culturing of the oocytes, injection of cRNA and defolliculation was performed as described by Sigel (1987). Oocytes were injected with 50 nl RNA solution, RNA coding for Hco-DEG-3 and Hco-DES-2 at a ratio of 25 nM:100 nM. In case of the GABA$_A$ receptor, combinations of α_1, β_2 and γ_2 subunits were expressed at a ratio of 10 nM:10 nM:50 nM (Boileau et al., 2002). The injected oocytes were incubated in modified Barth's solution at 18°C for about 72 h for the detailed characterization of the functional receptors.

Two-electrode voltage-clamp measurements. Unless indicated otherwise, measurements were done in medium containing 90 mM NaCl, 1 mM MgCl$_2$, 1 mM KCl, 1 mM CaCl$_2$ and 5 mM HEPES pH 7.4 at a holding potential of –80 mV. Currents were measured using a custom-made two-electrode voltage clamp amplifier in combination with a XY-recorder (90% response time 0.1s) or digitized at 100 Hz using a MacLab/200 (AD Instruments). The amplifier was characterized by a linear response up to 20 µA. Agonist was applied in absence or presence of modulatory compounds for

20 sec. The modulatory compounds were prepared as a 10 mM stock solution in dimethylsulfoxide (DMSO) and were dissolved in external solution resulting in a maximal final DMSO concentration of 0.1%. The perfusion solution (6 ml/min) was applied through a glass capillary with an inner diameter of 1.35 mm, the mouth of which was placed about 0.4 mm from the surface of the oocyte enabling 70% solution change in 0.5 sec (Baur and Sigel, 2007). Concentration response curves for choline were fitted with the equation $I(c)=I_{max}/(1+(EC_{50}/c)^n)$, where c is the concentration of choline, EC_{50} the concentration of choline eliciting half maximal current amplitude, I_{max} is the maximal current amplitude, I the current amplitude and n the Hill coefficient.

Relative current potentiation by AAD derivatives was determined as $(I_{1\ \mu M\ AAD\ +\ 1\ mM\ choline} / I_{1\ mM\ choline} - 1) * 100\%$. Data are given as mean $\pm$ SEM. The perfusion system was cleaned between two experiments by washing with 100% DMSO after application of AAD derivatives to avoid contamination.

RESULTS

Cloning of H. contortus predicted nAChR subunits and Hco-RIC-3. In search of a monepantel-sensitive channel from *Haemonchus contortus*, we aimed to functionally express in *Xenopus laevis* oocytes predicted nAChR subunits of the DEG-3 subfamily such as *Hco-mptl-1* and *Hco-des-2* (which had been implicated in AAD susceptibility), and *Hco-deg-3* (which is on the same operon as *Hco-des-2*). We also identified a *H. contortus* homologue of RIC-3 (resistant to inhibitors of cholinesterase) an ER-resident chaperone which was shown to enhance the expression of functional acetylcholine receptors at the cell surface in *C. elegans* (Halevi et al., 2002). A tblastn search (Altschul et al., 1990) with RIC-3 as the query against the (incomplete) *H.*

contortus genome database (www.sanger.ac.uk/Projects/H_contortus) returned as the best hit supercontig_0059267, containing coding sequences for a *H. contortus* RIC-3 homologous protein named Hco-RIC-3. Gene-specific primers were designed to obtain the complete open reading frame via RACE-PCR. The predicted protein Hco-RIC-3 consists of 365 amino acids with 65% similarity (Needleman-Wunsch global alignment) to *C. elegans* RIC-3 and carries the hallmarks of RIC-3 type chaperones: two transmembrane domains (as predicted by Phobius; Käll et al., 2004) followed by two coiled-coil domains (as predicted by COILS; Lupas et al., 1991), and a high proportion of charged amino acids: 66 negative (aspartate or glutamate) and 64 positive (arginine or lysine; Supplementary Figure S1). The full-length coding sequences of all genes were cloned into *E. coli* expression plasmids.

Functional expression in Xenopus oocytes – pilot experiments. The cloned *H. contortus* genes were transcribed in vitro, 5' capped, 3' polyadenylated, purified, and injected into *Xenopus laevi*s oocytes. After 72 h, currents were elicited by addition of acetylcholine or choline. Injection of *Hco-mptl-1*, with or without *Hco-ric-3*, produced no detectable currents. Injection of *Hco-deg-3* or *Hco-des-2* alone resulted in very small currents, which were not enhanced by co-injection of *Hco-ric-3* (Table 1). Stronger currents were obtained from the combined expression of *Hco-deg-3* and *Hco-des-2*, injected at a ratio of 1:1 (200 nM each). Bias of the channel towards Hco-DES-2 by decreasing the ratio of *Hco-deg-3* to *Hco-des-2* to 1:4 (25:100 nM) promoted the late, non-desensitising phase of the current (which turned out to be the pharmacologically more interesting; see below). This combination resulted in a peak current amplitude of 161 ± 101 nA (n = 24) and residual current after 20 sec of agonist application (1 mM choline) of 18 ± 9 nA (n = 24). Co-expression with *Hco-ric-3* decreased the initial rapid

transient current and increased the late current phase about two-fold (Table 1). Co-injection of *Hco-mptl-1*, with or without *Hco-ric-3*, did not significantly affect the current amplitudes or desensitization properties of Hco-DEG-3/Hco-DES-2 channels (not shown).

Choline is the preferred agonist of H. contortus DEG-3/DES-2 channels. Choline proved to be a much more potent agonist of the H. contortus DEG-3/DES-2 channels than acetylcholine. 10 mM acetylcholine elicited only $15.7 \pm 3.6\%$ (n = 4) of the current amplitude elicited by 1 mM choline (Figure 1), even though choline at 1 mM elicited only a small percentage of the maximal current (Figure 2B). An individual concentration response curves with choline as agonist obtained from oocytes expressing Hco-DEG-3/Hco-DES-2 channels are shown in Figure 2A. Each curve was fitted to the equation given under Methods and normalized to the fitted maximal current amplitude. The averaged curve for choline (Figure 2B) was characterized by an EC_{50} of 9.9 ± 2.5 mM choline and a Hill coefficient of 1.34 ± 0.13 (n = 4), indicating the presence of more than one agonist binding site per receptor. These values were obtained from peak current amplitudes. At concentrations >0.5 mM choline, desensitization was very fast. The decaying current traces were therefore back-extrapolated to half-maximal rise-time of the current trace to obtain corrected current amplitudes. Neither EC_{50} nor the Hill coefficient resulting from the corrected concentration response curves was significantly different from the values obtained directly (not shown). Figure 2B also shows a concentration response curve for acetylcholine standardized to the maximal current amplitude achieved in the same oocytes with choline.

Ion selectivity of H. contortus DEG-3/DES-2 channels. The currents elicited by addition of 1 mM choline to Hco-DEG-3/Hco-DES-2 expressing oocytes were

recorded in standard medium (1 mM $CaCl_2$), low calcium medium (standard medium without $CaCl_2$ plus 0.1 mM K-EGTA), and high calcium medium (standard medium supplemented with 8 mM $CaCl_2$). The amplitude of the rapid transient current and the rate of desensitization were strongly dependent on the Ca^{2+} concentration (Figure 3). At low $[Ca^{2+}]$, peaks were 28 ± 32% (n = 4) larger and the rate of desensitization was slower than compared to standard medium. At high $[Ca^{2+}]$, peaks were 60 ± 7% (n = 4) smaller and the rate of desensitization was faster. The lower peak amplitude observed at higher $[Ca^{2+}]$ could not be explained by an artefact caused by very rapid desensitization, as exponential back-extrapolation (not shown) indicated a real decrease in current amplitude.

Instantaneous I-V curves were recorded from the *H. contortus* DEG-3/DES-2 channels after the initial fast phase of desensitization. The reversal potential of the current elicited by 1 mM choline was -4 ± 2 mV (n = 4) in low calcium medium, -7 ± 2 mV (n = 4) in standard medium, and -24 ± 1 mV (n = 4) in high calcium medium. The reversal potential for chloride ions was determined as -30 ± 3 mV (n = 3), monitoring current through recombinant $\alpha_5\beta_2\gamma_2$ $GABA_A$ receptor channels. Thus, in the presence of high $[Ca^{2+}]$ the reversal potential of *H. contortus* DEG-3/DES-2 channels approached that of Cl^-. Similar observations had been made for *C. elegans* DEG-3/DES-2 channels, where intracellular sequestration of Ca^{2+} with a chelating agent prevented the shift in the reversal potential (Yassin et al., 2001). Presumably, the DEG-3/DES-2 channel is slightly permeable to calcium ions which in turn activate the Ca^{2+}-dependent Cl^- channel endogenous to *Xenopus* oocytes (Barish, 1983).

Modulation of H. contortus DEG-3/DES-2 channels by monepantel. Amino-acetonitrile derivatives alone, added at 30 µM to Hco-DEG-3/Hco-DES-2 expressing

oocytes, failed to elicit any current by themselves (not shown). Monepantel sulfone

(AD-4670) was tested at 0.1 μM, 0.3 μM, 1 μM, 3 μM, 10 μM and 30 μM. In all cases

less than 4 nA current were elited (n = 3). However, the AADs potentiated the currents

elicited by choline. Figure 4A shows current traces of a concentration-response curve

with monepantel sulfone (AD-4670) at 1 mM choline. 1 mM choline alone elicited 100-

190 nA. While slightly decreasing the amplitude of the initial rapid transient current,

monepantel sulfone strongly enhanced the subsequent, non-desensitizing current.

Averaged concentration response curves of this late current (steady-state current,

determined 20 sec after addition of choline) after normalization of the individual curves

to the current amplitude measured at 10 μM monepantel sulfone, were characterized by

an EC_{50} of 3.6 ± 2.9 μM (n = 5) monepantel sulfone and a maximal potentiation of

about 540% (Figure 4B). Monepantel at 10 μM had a smaller maximal effect on the late

current response of about 130% (n = 4). Co-injection of *Hco-mptl-1* cRNA, with or

without *Hco-ric-3*, did not significantly affect the modulation of *H. contortus* DEG-

3/DES-2 channels by monepantel (not shown). Interestingly, the optical R-enantiomer

of monepantel (AAD-2224) which fails to immobilize nematodes, was not simply

inactive but oppositely affected *H. contortus* DEG-3/DES-2 channels with a significant

inhibition of the current response to about 25% (n = 5) when applied at 10 μM (Figure

4C). The IC_{50} of AAD-2224 was similar to the EC_{50} of monepantel sulfone (AD-4670).

The AAD-mediated potentiation of the current was measured at a concentration

of 1 mM choline, which elicits only a small fraction of the maximal current amplitude

(Figure 2B). We recorded choline concentration response curves in the presence of 10

μM monepantel sulfone (AD-4670). To allow comparison with the curve obtained in

the absence of drug, the experiment was preceded by an application of 1 mM choline

alone. All current amplitudes were normalized to the current amplitude elicited by 1 mM choline. The averaged curves for the peak current amplitudes in the absence or presence of 10 µM monepantel sulfone (AD-4670) were characterized by an EC_{50} of 11.9 ± 2.5 mM and 9.9 ± 2.5 mM choline, respectively, and the same Hill coefficient of 1.3 ± 0.1 (Figure 5A). While the residual current amplitude, determined 20 sec after addition of the agonist (steady-state current), did not saturate within the range of choline concentrations tested, the response was strongly potentiated by monepantel sulfone (10 µM) over the entire choline concentration range (Figure 5B). Monepantel sulfone (AD-4670) even activated Hco-DEG-3/Hco-DES-2 channels after extensive desensitization: 10 µM was applied in combination with 1 mM choline after exposure for 30 sec to the same concentration of choline (Figure 5C). Activation of the current was clearly seen but characterized by a slow onset. In three experiments, the mean potentiation at the end of drug application was $361 \pm 46\%$.

Testing of further amino-acetonitrile derivatives. A panel of selected amino-acetonitrile derivatives was tested for their modulatory effects on *H. contortus* DEG-3/DES-2 channels. Each compound was applied at 1 and 10 µM. The eleven different AADs were highly active in vitro against *H. contortus* (Kaminsky et al., 2008b) and all of them affected the currents mediated by 1 mM choline, while nitenpyram, a neonicotinoid that activates insect nAChR's, had no effect on the *Haemonchus* channel (Figure 6). However, the tested AADs did not exhibit consistent activity: compounds 2-7 inhibited the late current and compounds 8-12 potentiated it (Figure 6). Note that these AADs were applied as racemic mixtures since we do not have them as pure enantiomers.

AAD derivatives have a minor effect on recombinant $\alpha_1\beta_2\gamma_2$ GABA$_A$ receptors. To test whether AADs have an effect on other channels of the Cys-loop family we used oocytes expressing recombinant human $\alpha_1\beta_2\gamma_2$ GABA$_A$ receptors. 1 µM monepantel had no effect on the current response with -2 ± 3% (n = 3), while 10 µM resulted in allosteric potentiation amounting to 30 ± 10% (n = 3). 10 µM of the inactive enantiomer of monepantel, AAD-2224, did not significantly affect the current responses with 2 ± 7% (n = 3). 10 µM of monepantel sulfone had a small effect on EC$_{50}$ responses to GABA with relative currents amounting to of -6 ± 1% (n = 3).

DISCUSSION

The DEG-3 subfamily is a clade of predicted acetylcholine receptors that only occurs in nematodes. The proteins carry the hallmarks of nicotinic AchR alpha-subunits such as the cysteine-cysteine pair in the N-terminal extracellular domain which is essential for agonist binding. However, the physiological role of these receptors remains

15

to be elucidated. So far, the only member of the subfamily whose function was addressed experimentally has been the DEG-3/DES-2 channel of *C. elegans*. Fusion of GFP or LacZ to either subunit localized the channel to the M1 head muscles, inner labial-2 (IL-2) neurons, flap (FLP) neurons, posterior ventral D (PVD) neurons, and posterior ventral C (PVC) neurons (Treinin et al., 1998). The DEG-3/DES-2 channel was suggested to play a role in chemosensation to the agonist, which turned out to be choline rather than acetylcholine (Yassin et al., 2001). The *H. contortus* DEG-3/DES-2 receptors, too, are activated only inefficiently by acetylcholine but strongly by high concentrations of choline (Figure 1). The elicited current is characterized by a rapid transient peak and a relatively small residual phase after desensitization (Figure 2). The action of Ca^{2+} is complex. Increases in $[Ca^{2+}]$ strongly decrease peak current amplitudes (Figure 3) as well as currents determined after exposure for 20 sec to agonist (late currents). Ca^{2+} ions also seem to penetrate the channel to a small extent as indicated by the shift of the reversal potential from near zero towards the equilibrium potential of Cl^- ions. Ca^{2+} ions are known to activate a Ca^{2+}-dependent Cl^- channel endogenous to *Xenopus* oocytes (Barish, 1983). Thus the *H. contortus* DEG-3 and DES-2 proteins are highly similar to the *C. elegans* orthologues DEG-3 and DES-2, respectively, and the *H. contortus* DEG-3/DES-2 receptor channel expressed in *Xenopus* oocytes exhibits similar electrophysiological properties to the *C. elegans* DEG-3/DES-2 receptor channel. However, *H. contortus* loss-of-sensitivity mutants to monepantel carried mutations in *Hco-des-2* (Kaminsky et al., 2008a; Rufener et al., 2009), but a *C. elegans deg-3(u662) des-2(u695)* double mutant was as sensitive to AADs as the corresponding wild-type (Kaminsky et al., 2008a). Furthermore, monepantel against *H. contortus* causes paralysis of the body musculature, leaving the head and tail regions motile, but

the *C. elegans deg-3/des-2* genes are expressed exactly in the head and the tail (Treinin et al., 1998). In summary, while the physiology of *C. elegans* and *H. contortus* DEG-3/DES-2 receptor channels may be similar, their pharmacology is not. The *Xenopus* expression system might be helpful to resolve this discrepancy. Of particular interest would be the functional analysis of mixed receptors consisting of *C. elegans* and *H. contortus* subunits, or even *C. elegans - H. contortus* chimeric subunits.

So far, direct evidence for interaction of AAD with receptor channels of the DEG-3 subfamily has been missing. Here we demonstrate that monepantel sulfone (AD-4670), the major metabolite of monepantel in sheep (Karadzovska et al., 2009), potentiates the choline-activated currents mediated by *H. contortus* DEG-3/DES-2 receptors in a concentration-dependent way (Figure 4) without opening the channels by itself. Thus, it acts as a positive allosteric modulator with a threshold of about 0.3 μM and an EC_{50} of about 4 μM. Allosteric modulators of the nicotinic acetylcholine receptor have been classified into type I and type II modulators (Bertrand and GopalaKrishnan, 2007). Type I modulators predominantly affect peak current amplitudes and type II modulators predominantly affect the time course of agonist-induced currents. The fact that it potentiates late currents and activates the desensitized channel (Figure 5) clearly classifies monepantel sulfone (AD-4670) as a type II positive allosteric modulator. Since the *H. contortus* DEG-3/DES-2 channel has some Ca^{2+} permeability, monepantel could, by promoting late current amplitudes of the channel, cause an increase of cytosolic $[Ca^{2+}]$ upon prolonged exposure to choline.

Monepantel (AAD-1566) and AAD-2224 are optical enantiomers, S and R respectively (Ducray et al. 2008), the former being almost 1000-fold more active against *H. contortu*s than the latter. Interestingly, the two enantiomers affect *H.*

contortus DEG-3/DES-2 channel function in opposite directions: while monepantel potentiates late currents, AAD-2224 inhibits them (Figure 4C). This property is highly unusual as generally one of the isomers of a chiral drug is inactive. The only similar case known to us is the dihydropyridine Sandoz 202-791, the isomer (+)-(S)-202-791 potentiating L-type Ca^{2+} currents, the other isomer (-)-(R)-202-791 inhibiting them (Reuter et al., 1988).

Two observations argue against *H. contortus* DEG-3/DES-2 receptor channels being the primary target of AAD anthelmintic action. First, *H. contortus* mutants selected for reduced susceptibility to AAD carried mutations not only in *Hco-des-2* but also in *Hco-mptl-1* (Rufener et al., 2009), but we found no evidence for an incorporation of Hco-MPTL-1 into Hco-DEG-3/Hco-DES-2 receptors. Second, the AADs exhibited in vitro activity against *H. contortus* at 0.01 ppm or lower (<30 nM), whereas the threshold of action on Hco-DEG-3/Hco-DES-2 receptors was about 300 nM. Nevertheless, the DEG-3/DES-2 channels may be of pharmacological interest as broad-spectrum anthelmintic drug targets. All nematodes analysed so far possess DEG-3 and DES-2 orthologues, including the human pathogenic ones such as filarial nematodes which lack MPTL-1 orthologues (Williamson et al., 2007). There are several possible reasons for the apparent lack of function of Hco-MPTL-1 in *Xenopus* oocytes. Not having antibodies against Hco-MPTL-1, we cannot test whether the injected *Hco-mptl-1* mRNA was properly translated; and even if, the resulting protein could be mis-folded or mis-localized in oocytes. Expression of Hco-MPTL-1 receptor channels might require a chaperone other than Hco-RIC-3. Furthermore, Hco-MPTL-1 might co-asssemble with other members of the large family of *H. contortus* putative AChRs to produce a functional receptor channel. Lastly, we cannot exclude the possibility that a

Hco-MPTL-1 receptor channel actually was expressed in a functional form, but that it requires a different agonist. Besides acetylcholine and choline, we have tested γ-aminobutyric acid, glutamate, glycine, kainic acid, urea, ethanolamine and serotonin on *Hco-deg-3* / *Hco-des-2* / *Hco-mptl-1* injected oocytes – to no avail.

In humans, nicotinic acetylcholine receptors are implicated in Alzheimer's disease, mild cognitive impairment, schizophrenia and attention deficit hyperactivity disorders. It would be interesting to see if some of the AADs penetrate the blood-brain barrier and modulate human brain nicotinic acetylcholine receptors. The fact that mammals tolerate high doses of monepantel and monepantel sulfone indicates that these compounds either do not penetrate the blood-brain barrier, or do not affect mammalian brain nicotinic acetylcholine receptors. In case the compounds reached the brain, our data indicate that the major inhibitory neurotransmitter receptor, the GABA$_A$ receptor, would remain unaffected. As monepantel is rapidly converted to the sulfone in vivo (Karadzovska et al., 2009), the fact that 10 μM monepantel slightly affected GABA$_A$ receptors is probably of little significance.

In conclusion, we provide the first direct evidence of interaction of AADs with their presumed targets, (acetyl)choline receptors of the nematode-specific DEG-3 subfamily. How the allosteric activation of *H. contortus* DEG-3/DES-2 channels by monepantel and monepantel sulfone contributes to the observed immobilization and killing of the parasites, and which role Hco-MPTL-1 plays therein, remains to be elucidated.

Acknowledgments

We are grateful to Jacques Bouvier for providing the compounds used in Figure 6. We thank Verena Niggli, Barry Hosking and Arthur Redpath for helpful comments on the manuscript.

References

Altschul S., Gish W, Miller W, Myers EW, andLipman DJ (1990) Basic local alignment search tool. *J. Mol. Biol.* **215**: 403-410.

Baur R, and Sigel E (2007) Replacement of histidine in position 105 in the α5 subunit by cysteine stimulates zolpidem sensitivity of α5β2γ2 GABA$_A$ receptors. *J. Neurochem.* **103**: 2556-2564.

Barish ME (1983) A transient calcium-dependent chloride current in the immature Xenopus oocyte. *J. Physiol.* **342**: 309-325.

Beech RN, Wolstenholme AJ, Neveu C, and Dent JA (2010) Nematode parasite genes: what's in a name? *Trends Parasitol.* **26**: 334-340.

Ben-Ami HC, Yassin L, Farah H, Michaeli A, Eshel M, and Treinin M (2005) RIC-3 affects properties and quantity of nicotinic acetylcholine receptors via a mechanism that does not require the coiled-coil domains. *J. Biol. Chem.* **280**: 28053-28060.

Bertrand D, and Gopalakrishnan M (2007) Allosteric modulation of nicotinic acetylcholine receptors. *Biochem. Pharmacol.* **74**: 1155-1163.

Blake N, and Coles G (2007) Flock cull due to anthelmintic-resistant nematodes. *Vet. Rec.* **161**: 36.

Boileau AJ, Baur R, Sharkey LM, Sigel E, and Czajkowski, C. (2002) The relative amount of cRNA coding for γ2 subunits affects potentiation by benzodiazepines in GABA$_A$ receptors expressed in Xenopus oocytes. *Neuropharmacology* **43**: 695-700.

Coles GC (1998) Drug-resistant Parasites of sheep:an emerging problem in the UK? *Parasitol. Today* **14**: 86-88.

Ducray P, Gauvry N, Pautrat F, Goebel T, Fruechtel J, Desaules Y, Weber SS, Bouvier J, Wagner T, Froelich O, and Kaminsky R (2008) Discovery of amino-acetonitrile

derivatives, a new class of synthetic anthelmintic compounds. *Bioorg. Med. Chem. Lett.* **18**: 2935-2938.

Halevi S, McKay J, Palfreyman M, Yassin L, Eshel M, Jorgensen E, and Treinin M (2002) The C. elegans ric-3 gene is required for maturation of nicotinic acetylcholine receptors. *EMBO J.* **21**: 1012-1020.

Holden-Dye L, and Walker RJ (2007) Anthelmintic drugs. WormBook, 1-13.

Käll L, Krogh A, and Sonnhammer EL (2004) A combined transmembrane topology and signal peptide prediction method. *J. Mol. Biol.* **338**: 1027-1036.

Kaminsky R, Ducray P, Jung M, Clover R, Rufener L, Bouvier J, Weber SS, Wenger A, Wieland-Berghausen S, Goebel T, Gauvry N, Pautrat F, Skripsky T, Froelich O, Komoin-Oka C, Westlund B, Sluder A, and Maser P (2008a) A new class of anthelmintics effective against drug-resistant nematodes. *Nature* **452**: 176-180.

Kaminsky R, Gauvry N, Schorderet WS, Skripsky T, Bouvier J, Wenger A, Schroeder F, Desaules Y, Hotz R, Goebel T, Hosking BC, Pautrat F, Wieland-Berghausen S, and Ducray P (2008b) Identification of the amino-acetonitrile derivative monepantel (AAD 1566) as a new anthelmintic drug development candidate. *Parasitol. Res.* **103**: 931-939.

Kaplan RM (2004) Drug resistance in nematodes of veterinary importance: a status report. *Trends Parasitol.* **20**: 477-481.

Karadzovska D, Seewald W, Browning A, Smal M, Bouvier J, and Giraudel JM (2009) Pharmacokinetics of monepantel and its sulfone metabolite, monepantel sulfone, after intravenous and oral administration in sheep. *J. Vet. Pharm. Ther.* **32**: 359-367.

Love SC, Neilson FJ, Biddle AJ, and McKinnon R (2003) Moxidectin-resistant Haemonchus contortus in sheep in northern New South Wales. *Aust. Vet. J.* **81**: 359-360.

Lupas A, Van Dyke M, and Stock J (1991) Predicting coiled coils from protein sequences. *Science* **252**: 1162-1164.

Reuter H, Porzig H, Kokubun S, and Prod'hom B (1988) Calcium channels in the heart. Properties and modulation by dihydropyridine enantiomers. *Ann. N. Y. Acad. Sci.* **522**: 16-24.

Rufener L, Maser P, Roditi I, and Kaminsky R (2009) Haemonchus contortus acetylcholine receptors of the DEG-3 subfamily and their role in sensitivity to monepantel. *PLoS Pathog.* **5**: e1000380.

Sargison ND, Jackson F, Bartley DJ, and Moir AC (2005) Failure of moxidectin to control benzimidazole-, levamisole- and ivermectin-resistant Teladorsagia circumcinda in a sheep flock. *Vet. Rec.* **156**: 105-109.

Sigel E (1987) Properties of single sodium channels translated by Xenopus oocytes after injection with messenger ribonucleic acid. *J. Physiol.* **386**: 73-90.

Sutherland IA, Damsteegt A, Miller CM, and Leathwick DM (2008) Multiple species of nematodes resistant to ivermectin and a benzimidazole-levamisole combination on a sheep farm in New Zealand. *New Zeal. Vet. J.* **56**: 67-70.

Traversa D, Paoletti B, Otranto D, and Miller J (2007) First report of multiple drug resistance in trichostrongyles affecting sheep under field conditions in Italy. *Parasitol. Res.* **101**: 1713-1716.

Treinin M, Gillo B, Liebman L, and Chalfie M (1998) Two functionally dependent acetylcholine subunits are encoded in a single Caenorhabditis elegans operon. *Proc. Natl. Acad. Sci. U S A* **95**: 15492-15495.

Waghorn TS, Leathwick DM, Rhodes AP, Lawrence KE, Jackson R, Pomroy WE, West DM, and Moffat JR (2006) Prevalence of anthelmintic resistance on sheep farms in New Zealand. *New Zeal. Vet. J.* **54**: 271-277.

Williamson SM, Walsh TK, and Wolstenholme AJ (2007) The cys-loop ligand-gated ion channel gene family of Brugia malayi and Trichinella spiralis: a comparison with Caenorhabditis elegans. *Invert. Neurosci.* **7**: 219-226.

Wrigley J, McArthur M, McKenna PB, and Mariadass B (2006) Resistance to a triple combination of broad-spectrum anthelmintics in naturally-acquired Ostertagia circumcincta infections in sheep. *New Zeal. Vet. J.* **54**: 47-49.

Yassin L, Gillo B, Kahan T, Halevi S, Eshel M, and Treinin M (2001) Characterization of the deg-3/des-2 receptor: a nicotinic acetylcholine receptor that mutates to cause neuronal degeneration. *Mol. Cell. Neurosci.* **17**: 589-599.

Yue C, Coles G, and Blake N (2003) Multiresistant nematodes on a Devon farm. *Vet. Rec.* **153**: 604.

Footnotes

[1]These authors contributed equally.

Legends for Figures

Fig. 1. Choline is the preferred agonist of *H. contortus* DEG-3/DES-2 channels. Hco-DEG-3/Hco-DES-2 channels were expressed in *Xenopus* oocytes. Three days after injection with RNA, currents were evoked with 10 mM acetylcholine and subsequently in the same oocyte with 1 mM choline. The membrane potential was held at –80 mV.

Fig. 2. Choline and acetylcholine concentration dependence. A) Current traces from a choline concentration response curve obtained from a *Xenopus* oocyte expressing Hco-DEG-3/Hco-DES-2 receptors. The bars indicate the time period of choline perfusion. Choline concentrations are indicated above the bars. B) Averaged choline and acetylcholine concentration response curves. Individual curves for choline were first normalized to the observed maximal current amplitude and subsequently averaged. Mean ± SD of experiments carried out with 3-4 oocytes from two batches are shown. Individual curves for acetylcholine were first normalized to the observed maximal current amplitude with choline in the same oocyte and subsequently averaged. Mean ± SD of experiments carried out with 3 oocytes are shown.

Fig. 3. Calcium ion concentration depedence of currents mediated by *H. contortus* DEG-3/DES-2 channels. Hco-DEG-3/Hco-DES-2 channels were exposed to 1 mM choline either in low calcium medium (standard medium with 1 mM $CaCl_2$ replaced by 0.1 mM K-EGTA, labelled 0.1 mM K-EGTA), standard medium (labelled 1 mM Ca^{2+}), and high calcium medium (standard medium supplemented with additional 8 mM $CaCl_2$, labelled 9 mM Ca^{2+}).

Fig. 4. AAD derivatives are channel modulators. A) Current traces from a cumulative concentration dependence of the potentiation by monepantel sulfone (AD-4670) of currents elicited by 1 mM choline obtained from a *Xenopus* oocyte expressing Hco-DEG-3/Hco-DES-2 receptors. The bars indicate the time period of choline or combined choline/monepantel sulfone (AD-4670) perfusion. Monepantel sulfone concentrations are indicated above the bars. B) Averaged monepantel sulfone (AD-4670) concentration response curve. Individual curves were first normalized to the observed maximal current potentiation and subsequently averaged. Mean ± SD of experiments carried out with 3-4 oocytes from two batches are shown. C) Averaged AAD-2224 and monepantel (AD-1566) concentration response curve.

Fig. 5. Monepantel sulfone (AD-4670) increases the late but not the peak current amplitude. Choline concentration response curves in the absence (open circles) and presence (closed circles) of 10 μM monepantel sulfone. Each experiment was preceded by an application of 1 mM choline in the absence of the modulatory compound. All current amplitudes were normalized to the current amplitude elicited by 1 mM choline that was assumed 100 %. A) peak current amplitudes, B) residual current after exposure of 20 sec to the agonist, C) Effect of monepantel sulfone (AD-4670) on the desensitized current component. 10 μM monepantel sulfone (AD-4670) was applied in combination with 1 mM choline after exposure for 30 s to the same concentration of choline.

Fig. 6. Screening of different AAD derivatives and nitenpyram for modulation of the late current after exposure for 20 sec to the agonist. A) Chemical structure of the tested

compounds. Extent of modulation by 1 μM (B) and 10 μM (C) of the compounds in the

presence of 1 mM choline.

Tables

Table 1

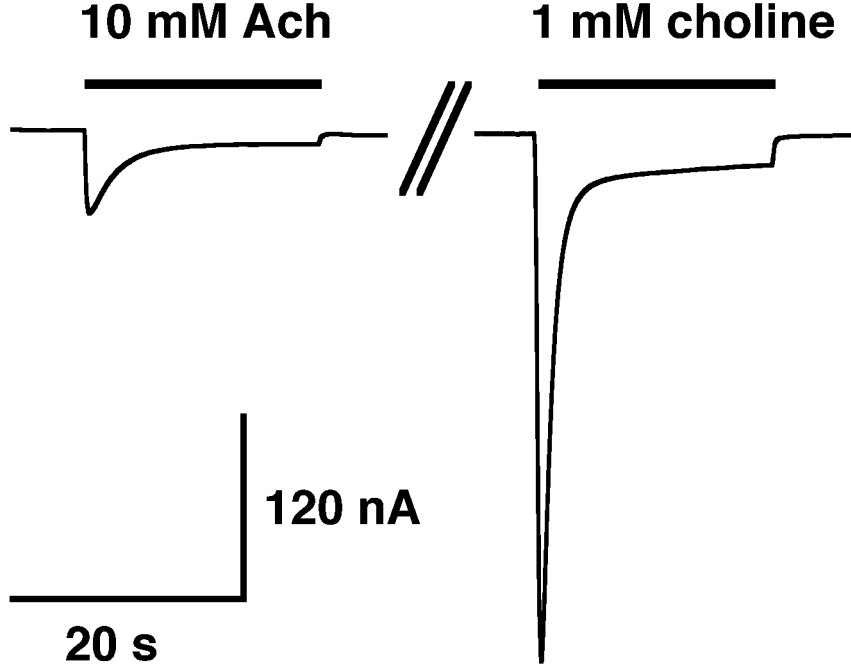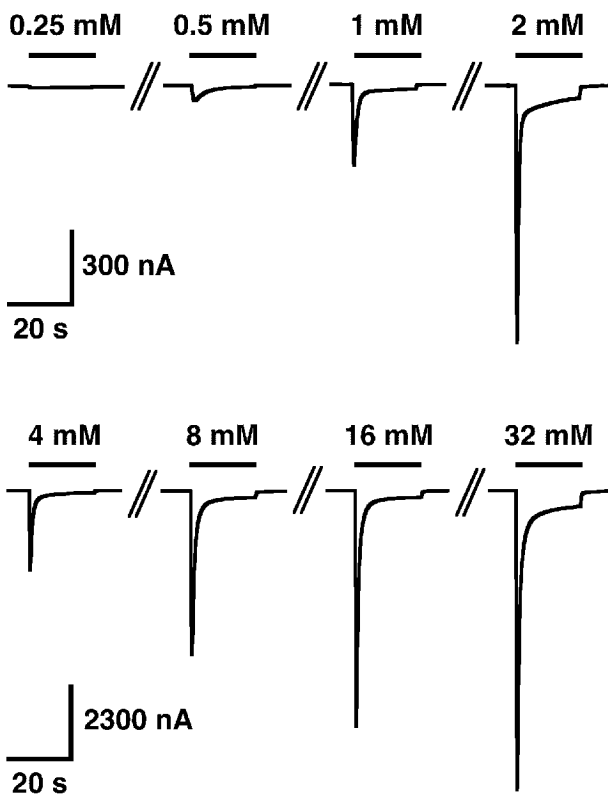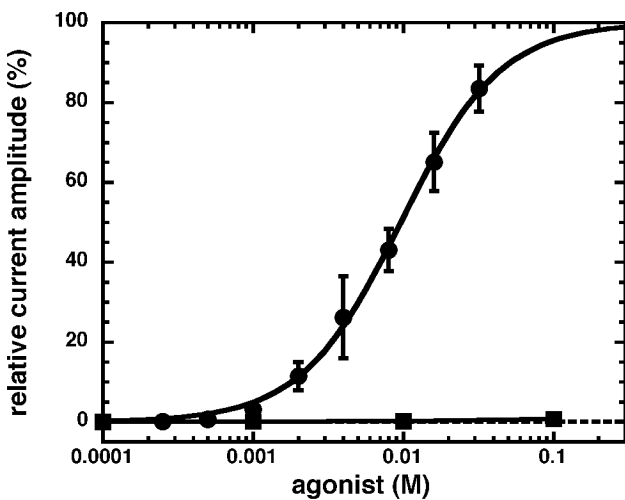| Receptor (fmol injected/oocyte)	Peak current (nA)	Tail current after 20 s (nA)
DEG-3 (1.25)	< 5	-
DEG-3 (1.25)/RIC-3 (5)	< 5	-
DES-2 (5)	< 5	-
DES-2 (1.25)/RIC-3 (5)	< 5	-
DEG-3 (1.25)/DES-2 (5)	161 ± 101 (24)	18 ± 9 (24)
DEG-3 (1.25)/DES-2 (5)/RIC-3 (5)	43 ± 37 (14)	34 ± 23 (14)

Hco-RIC-3 affects functional expression of *H. contortus* DEG-3/DES-2 channels

Peak current amplitudes were determined using 1 mM choline, 3 days after injection of *Xenopus* oocytes with the mentioned amounts of RNA. The number in bracket in column 2 and 3 is the number of oocytes.

10 mM Ach

1 mM choline

120 nA

20 s

Figure 1

A

0.25 mM   0.5 mM   1 mM   2 mM

300 nA

20 s

4 mM   8 mM   16 mM   32 mM

2300 nA

20 s

B

Figure 2

9 mM Ca^{2+} 1 mM Ca^{2+} 0.1 mM EGTA

1 mM ch.   1 mM ch.   1 mM ch.

30 nA

20 s

Figure 3

Figure 4

A

relative current potentiation (%)

choline (M)

B

relative current potentiation (%)

choline (M)

C

1 mM choline

10 μM AAD-4670
1 mM choline

60 nA

10 s

Figure 5

A
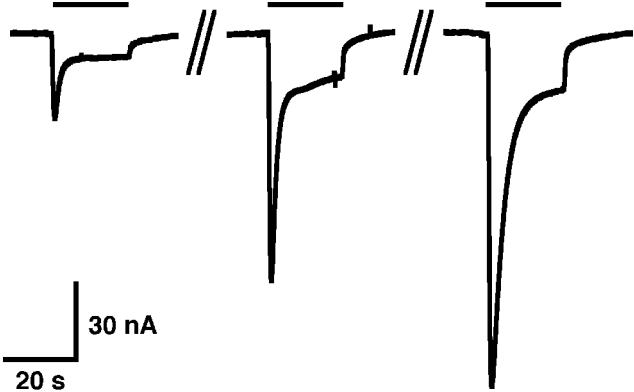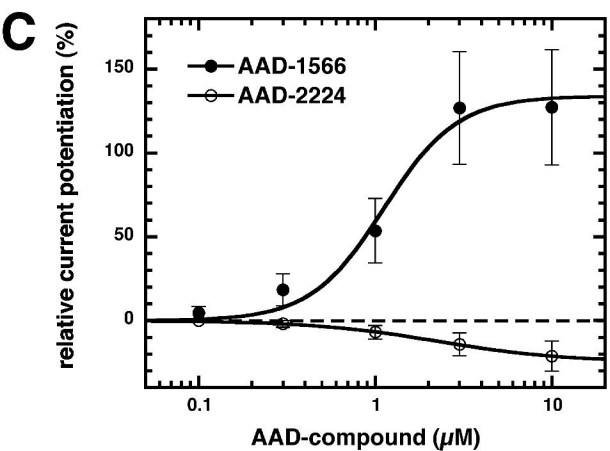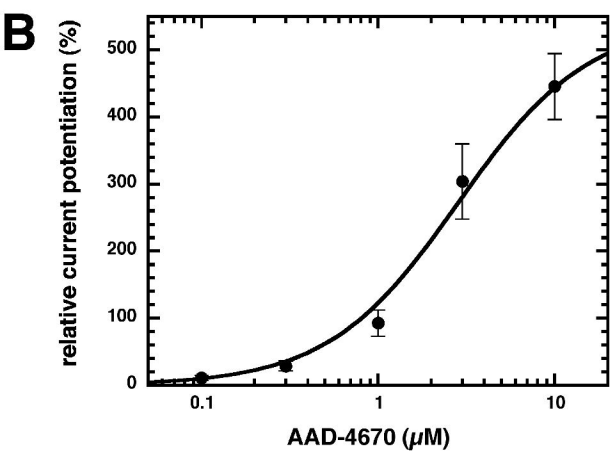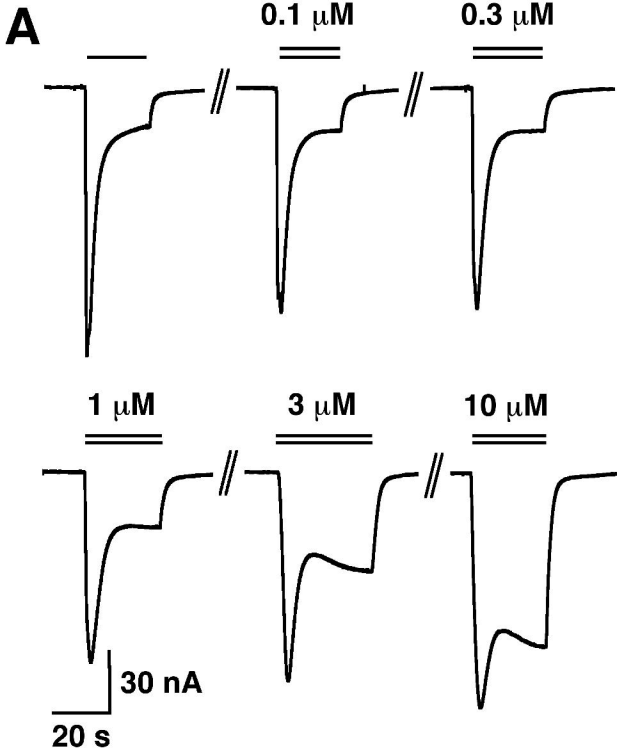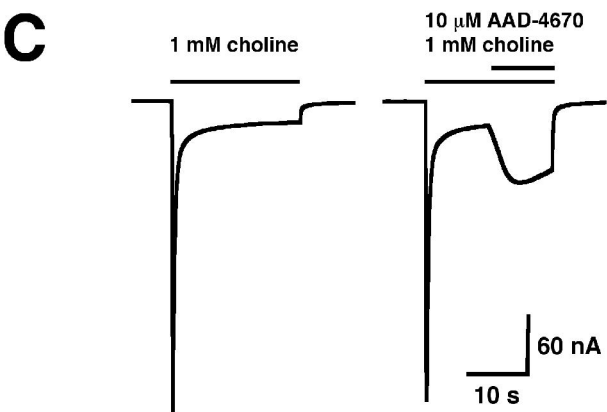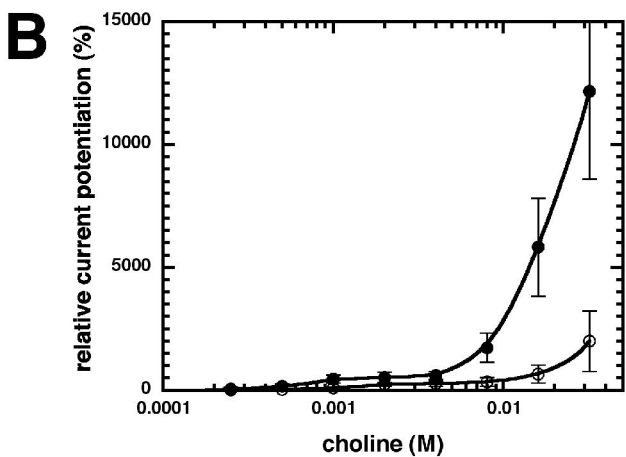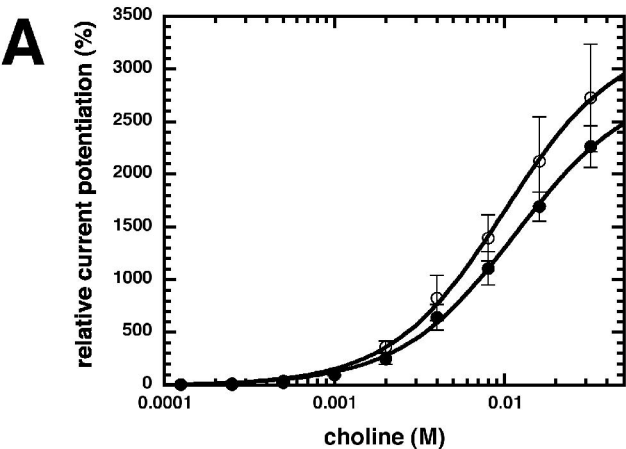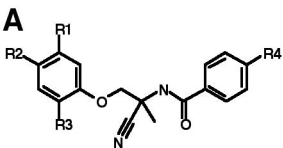
No.	name	R1	R2	R3	R4
0	AAD-4670	CN	H	CF_3	SO_2CF_3
1	nitenpyram				
2	AAD-0450r	H	H	Cl	CF_3
3	AAD-0907r	H	H	CF_3	CF_3
4	AAD-0970r	H	H	CF_3	OCF_3
5	AAD-1154r	Cl	H	Cl	OCF_3
6	AAD-1336r	F	F	Br	OCF_3
7	AAD-1470r	F	F	CF_3	OCF_3
8	AAD-0004r	F	F	Cl	OCF_3
9	AAD-2009r	H	F	Cl	OCF_3
10	AAD-1566r	CN	H	CF_3	SCF_3
11	AAD-4670r	CN	H	CF_3	SO_2CF_3
12	AAD-2105r	CN	H	CF_3	$SOCF_3$

Figure 6